BEC BIOENERGETICS COMMUNICATIONS
Bioenerg Commun 2024.8
https://doi.org/10.26124/bec.2024-0008
Open Access

Technical Communication

Cite
Baglivo E, Cardoso LHD, Cecatto C, Gnaiger E (2024) Stability of mitochondrial respiration medium used in high-resolution respirometry with living and permeabilized cells. Bioenerg Commun 2024.8. https://doi.org/10.26124/bec.2024-0008

Author contributions - CRediT
Conceptualization: EG
Data curation, formal analysis, methodology: EB, EG
Investigation: EB, LHDC, CC
Project administration, resources: EG
Supervision, validation: EG
Visualization, writing original draft: EB, EG
Review and editing: EB, EG, LHDC, CC

Conflicts of interest
EB, LHDC and CC are employees of Oroboros Instruments. EG is founder and CEO of Oroboros Instruments.

Received 2024-09-25
Reviewed 2024-11-04
Revised 2024-12-04
Accepted 2024-12-04
Published 2024-12-06

Open Peer Review
Alicia Kowaltowski (editor)
Jason Bazil (reviewer)
Debora Santos Rocha (reviewer)

Keywords
mitochondrial respiration medium;
cryopreserved HEK cells;
living and permeabilized cells;
quality control;
reproducibility

Stability of mitochondrial respiration medium used in high-resolution respirometry with living and permeabilized cells

Eleonora Baglivo, Luiza HD Cardoso, Cristiane Cecatto, Erich Gnaiger

Oroboros Instruments GmbH, Innsbruck, Austria

Corresponding authors: eleonora.baglivo@oroboros.at; erich.gnaiger@oroboros.at

Summary

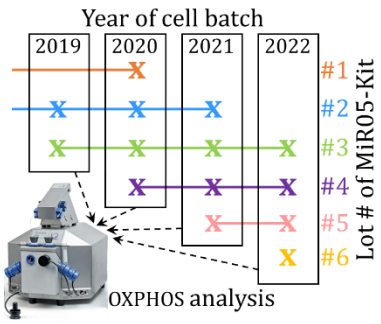

Quality control (QC) in mitochondrial respiration is essential to ensure accuracy and reproducibility at four levels: (*1*) sample preparation, (*2*) instrumental and technical performance, (*3*) data analysis, and (*4*) chemicals and respiration medium. In the present study, we focus on the quality of mitochondrial respiration medium MiR05, which plays a crucial role in supporting mitochondrial function.

We prepared MiR05 from 6 lots of MiR05-Kit with storage times of 1 to 51 months at room temperature. Two substrate-uncoupler-inhibitor titration (SUIT) reference protocols were used with cryopreserved HEK 293T cells in the Oroboros Bioenergetics Platform. These protocols interrogate 20 different respiratory states, of which four are comparable with the following rates: ROUTINE respiration of living cells; residual endogenous respiration after permeabilization by digitonin; electron transfer capacity with succinate, rotenone and glycerophosphate after uncoupler titration; and CIV activity stimulated by ascorbate and TMPD corrected for chemical O_2 background.

Respiration in all 20 respiratory states was reproducible between the lots of MiR05-Kit and independent of storage time up to 51 months. Chemical O_2 background – caused by autoxidation of cytochrome *c*, ascorbate and TMPD – was a linear function of O_2 concentration down to 50 µM and was comparable for each lot of MiR05-Kit and independent of storage time.

Our 4-year study demonstrates a constant quality of MiR05-Kit up to several years of storage. Stability of MiR05-Kit and consistency between different lots represent essential elements to obtain reproducible results with high-resolution respirometry in research and clinical investigations.

1. Introduction

A key function of mitochondria is to transduce energy stored in fuel substrates into the ATP hydrolysis potential. Accuracy and reproducibility of respiratory measurements rely on quality control (QC) on four levels: (*1*) Sample preparation, (*2*) instrumental and technical reproducibility, (*3*) data analysis, and (*4*) chemicals and respiration medium**.** Specifically, QC of respiration media plays a crucial role in mitochondrial respiration, as media are essential for supporting mitochondrial function.

For this reason, the choice and QC of an adequate respiration medium are fundamental in high-resolution respirometry (HRR). Different types of mitochondrial respiration media, with variable compositions, are currently in use, limiting the comparability of different studies (Doerrier et al 2024). On the one hand, the different formulations of respiration media do not facilitate the comparison between studies; on the other hand, even the same formulation may cause variability depending on the source of the used chemicals, and thus it does not guarantee comparable results. Therefore, the use of a standardized mitochondrial respiration medium becomes crucial to obtain consistent results.

Mitochondrial respiration medium MiR05 (Gnaiger et al 2000) is prepared from MiR05-Kit which is a dry powder stored at room temperature. The present study was designed to evaluate the consistent and constant quality of different lots of MiR05-Kit over storage times of up to four years. Considering the currently estimated expiration date for the closed vial of MiR05-Kit of two years, our data establish a retest date beyond this expiration date. Recommended retest dates include the period of time until which a chemical is expected to remain stable and match the default specifications if stored under the conditions specified by the manufacturer.

In the present study, we compared respirometric results obtained with six different lots of MiR05-Kit, with storage times at room temperature from 1 to 51 months. Measurements were performed using cryopreserved HEK 293T cells and two complementary substrate-uncoupler-inhibitor titration (SUIT) protocols. The analysis was particularly focused on respiratory states which are comparable in the two protocols and extended to precision OXPHOS analysis. In addition, the chemical background O_2 flux was analyzed.

2. Material and methods

2.1. Mitochondrial respiration medium MiR05

Mitochondrial respiration medium MiR05 is prepared from MiR05-Kit (Oroboros Instruments, product ID 60101-01). Each lot consists of seven homogeneously mixed components partitioned into vials (Table 1) and stored at room temperature. The dry MiR05-Kit powder may contain gray or black specks.

Table 1. Chemical composition of each vial of MiR05-Kit. The amounts are calculated for a final volume of 250 mL of aqueous solution.

MiR05 component	Molar mass [g·mol^{-1}]	Mass [g]	Concentration [mM]
EGTA	380.4	0.047	0.5
$MgCl_2$	95.2	0.071	3
Lactobionic acid	358.3 free acid	5.375	60
Taurine	125.1	0.625	20
KH_2PO_4	136.1	0.340	10
HEPES	238.3	1.191	20
D-Sucrose	342.3	9.413	110

MiR05 was prepared from the powder of one MiR05-Kit vial dissolved in 230 mL H_2O. The solution was stirred at 30 °C, 3.75 mL of 5 M KOH were added, and pH was adjusted to 7.1 at 30 °C using a pH electrode. Stepwise pH adjustment may require up to 90 min and the pH has to be stable for at least 5 min. Approximately 50 mL of this solution were added into a separate glass beaker and 0.25 g bovine serum albumin (BSA fatty acid free, Sigma-Aldrich A6003 fraction V, storage temperature 4 °C) were dissolved completely. This solution was combined with the main solution. pH was checked and re-adjusted to pH 7.1 at 30 °C if necessary. H_2O was added to a final volume of 250 mL (BSA 1 g·L^{-1}). The MiR05 solution was partitioned into appropriate aliquots in plastic vials and stored at -20 °C. The MiR05 solution might have a slight yellow coloring, which had no impact on respiration of isolated mitochondria and cryopreserved HEK cells.

We evaluated six lots of MiR05-Kit. The vials were stored for different times at room temperature as a crystalline powder. The MiR05 solutions were prepared approximately one week before each experiment and stored at -20 °C. Different lots of MiR05-Kit and their storage times are shown in Figure 1 for lots 0915 (#1), 18.02872 (#2), 19.01689 (#3), 20J01923 (#4), 21J01861 (#5), and 22J01040 (#6).

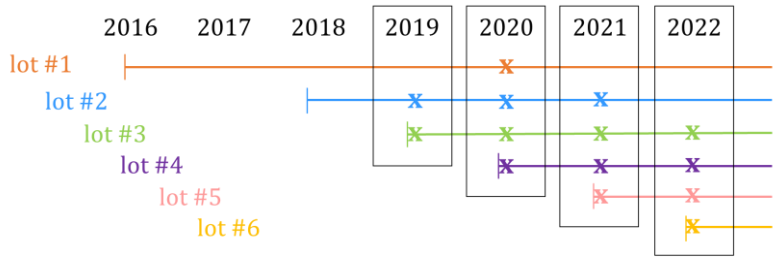

Figure 1. Storage times of 6 lots of MiR05-Kit. Storage times varied from 4 years (lot #1 in 2020) to less than 1 month (lots #3, #4, #5 and #6 in 2019, 2020, 2021, and 2022 respectively).

2.2. Chemicals

The following chemicals were used in the respirometric protocols (abbreviations, concentrations of stock solutions, and catalog number given in parentheses). From Sigma-Aldrich: cytochrome *c* (c, 4 mM; C7752); glutamate (G, 2 M; G1626), malate (M, 50 mM, and 400 mM; M1000), pyruvate (P, 2 M; P2256), succinate (S, 1M; S2378), carbonyl cyanide m-chlorophenyl hydrazone CCCP (U, 1 mM; C2759), antimycin A (Ama, 5 mM; A8674), rotenone (Rot, 1 mM; R8875), digitonin (Dig, 10 mg·mL^{-1}; D5628), ascorbate (As, 800 mM; A7631), *N,N,N′,N′*-tetramethyl-*p*-phenylenediamine dihydrochloride TMPD (Tm, 200 mM; T3134), sodium azide (Azd, 4 M; S2002). From Merck: ADP (D, 500 mM; 117105). From Santa Cruz Biotechnology: glycerophosphate (Gp, 1 M; sc-215789). From Biotrend (APExBIO Technology): octanoylcarnitine (Oct, 100 mM; B6371). Stock solutions were titrated with Hamilton microsyringes into the Oroboros chambers, adjusting the titration volumes to obtain the experimental concentrations indicated in the figure legends. For cell counting PBS (Phosphate-buffered saline, Sigma-Aldrich) was used. All solutions and media were prepared with deionized ultra-pure H_2O (Ultra Clear™ TP UV UF TM, Evoqua Water Technologies GmbH, resistivity at 25 °C 18.2 MΩ·cm). Ensuring water purity is essential to achieve consistent results.

2.3. Sample preparation

Experiments were performed with cryopreserved HEK 293T cells (Krumschnabel et al 2024), with different durations of cryopreservation (CR time) before experiments (Table 2). In every year of measurement, the same batch of HEK 293T cells was used such that results on an identical batch with the same cryopreservation time were compared within each year. Different batches were used in different years to avoid a possible effect of varying storage times of several years and considering the practically limited number of cryopreserved subsamples. Each batch is identified by the corresponding year of respiratory measurement (Table 2). The cells were harvested and cryopreserved in the lab of Oroboros Instruments (2019 and 2020) and the Institute of Biochemistry, University of Innsbruck (2021 and 2022). The number of cell passages before cryopreservation was between 3 and 10 for all batches.

Table 2. Cryopreservation (CR) time of HEK 293T cells. For each experimental day, the first two viability values represent independent measurements, and the third one represents their average.

Cell batch	Freezing date	CR time [months]	Viability [%]			
HEK 2019	2019-10-22	1	day 1	83	82	82.5
HEK 2020	2020-01-15	10	day 1	88	92	90
			day 2	93	90	91.5
HEK 2021	2021-05-04	6	day 1	88	95	91.5
			day 2	91	90	90.5
HEK 2022	2022-07-26	2	day 1	95	95	95
			day 2	90	90	90

Cell counting was performed as follows: (*1*) Cells were thawed by adding 500 µL PBS at room temperature to each vial and several vials were pooled; (*2*) 20 µL cell suspension were added to 180 µL PBS (1:10 dilution); (*3*) 15 µL of diluted sample was added to 15 µL Trypan Blue; (*4*) 10 µL of sample with Trypan Blue was added to each chamber of the disposable slides of the cell counter (Countess™ Cell Counter, Invitrogen, Waltham, MA, USA); (*5*) cells were counted after they settled for 2 min. After every dilution step, cells were mixed by several up-and-down cycles with a pipette. Calculation of the cell count added into the Oroboros chambers considered the total cell count and not the viability of the cells (Table 2).

2.4. High-resolution respirometry

All procedures were performed by experienced operators. Experiments were conducted in several Oroboros Bioenergetics Platforms in parallel. The oxygen solubility factor of MiR05 relative to pure water is 0.92 at 37 °C, applied for air calibration of the oxygen sensors (Gnaiger 2008). The cells were added to the Oroboros chambers by partial volume replacement (Leo et al 2024). After stopping the stirrers, the calculated volume of MiR05 was removed with a pipette from each chamber, and the same volume of cell suspension was added with the same pipette. For sample volume calculation, a chamber volume of 2.07 mL including the capillary was considered, yielding an effective experimental volume of 2.0 mL. The same operator added the cells to all chambers. Then the stirrers were re-started.

Two SUIT protocols were applied: reference protocol RP1 (Figure 2a and 2c) and RP2 (Figure 2b and 2d) (Timón-Gómez et al 2024). The chemical O_2 background test was performed in absence of biological sample (Section 3.2).

RP1 focuses on coupling control in the NADH-pathway, with pyruvate and malate, while RP2 gives information on the F-pathway in the OXPHOS state. OXPHOS capacity is measured in the presence of saturating ADP concentrations. Taken together, RP1 and RP2 cover 20 different pathway and coupling control states. These include four comparable respiratory states (Figure 2a and 2b):

1. *R* represents ROUTINE respiration of living cells;
2. *Ren* is respiration after addition of digitonin for permeabilization of plasma membranes;
3. SGp$_E$, ET state after succinate&glycerophosphate respiratory stimulation in the presence of rotenone;
4. CIV activity stimulated by ascorbate&TMPD, in the presence of cytochrome *c*. The protocols were carried out in MiR05 without catalase, although, in general, catalase is recommended to avoid accumulation of hydrogen peroxide during autoxidation of ascorbate&TMPD.

Comparable respiratory states are identical (*R* and *Ren*) or harmonized (SGp$_E$ and CIV) when the same effective SUIT chemicals are present after different titration sequences of the SUIT protocols (Timón-Gómez et al 2024).

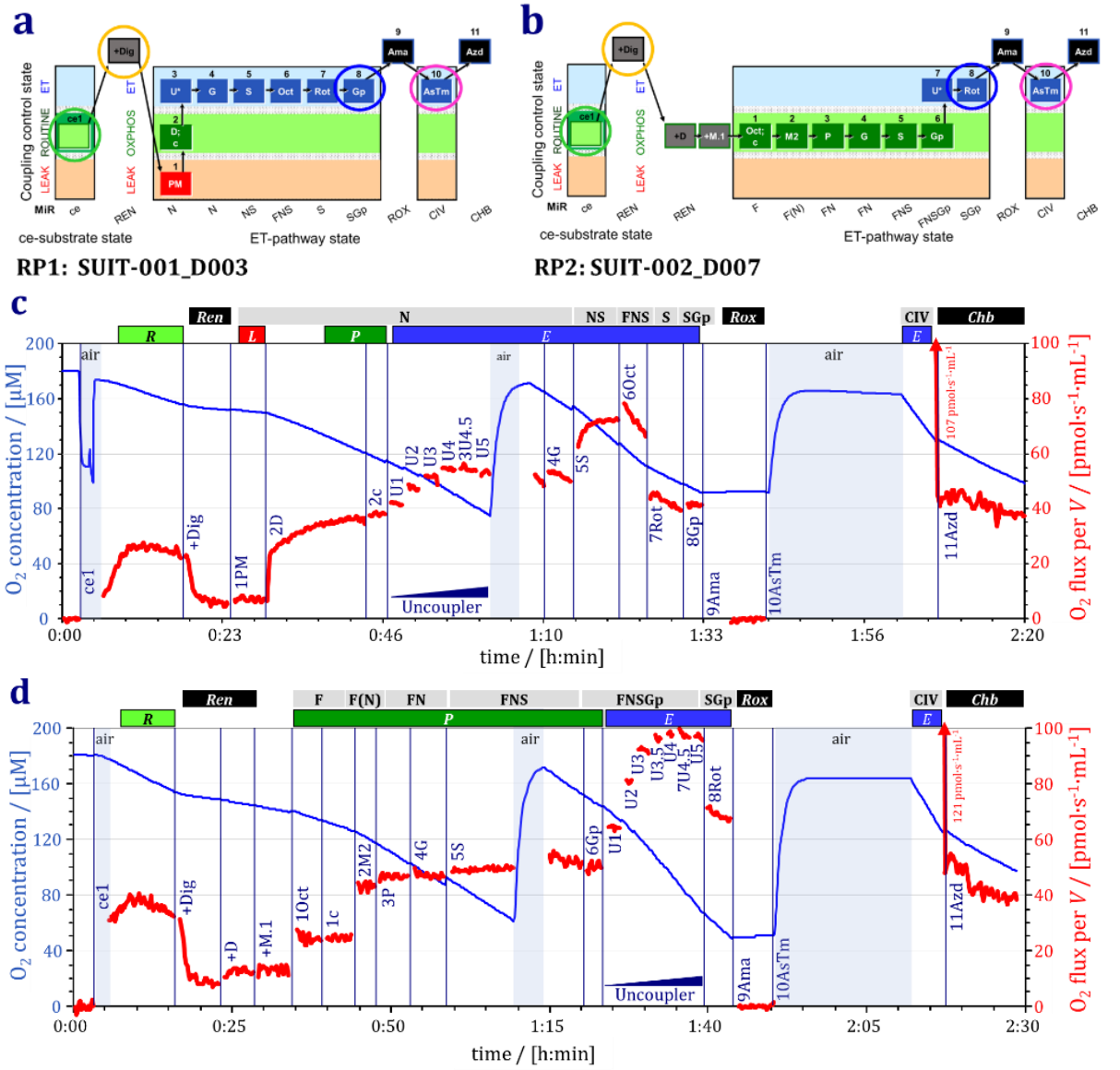

Figure 2. SUIT reference protocols. Coupling/pathway control diagrams (panels a and b) and representative traces (panels c and d) of O_2 concentration [µM] (blue lines) and volume-specific O_2 flux [pmol·s^{-1}·mL^{-1}] (red lines; corrected for instrumental background O_2 flux; spikes caused by titrations were eliminated). Oxygen concentration was kept above 60 µM by intermittent reoxygenations (air, open chamber, blue shade). RP1 and RP2 cover 20 different coupling and pathway control states in sequence, characterized by titrations and corresponding rates. **(a)** and **(c)** RP1 (SUIT-001_D003): **ce1**, ROUTINE respiration *R* of living cells. **+Dig**, digitonin 10 µg·mL^{-1}; permeabilization of plasma membranes (ce to pce), residual endogenous respiration *Ren*. **1PM**, pyruvate 5 mM & malate 2 mM; N-pathway LEAK respiration N_L. **2D**, ADP 2.5 mM; N-pathway OXPHOS capacity N_P. **2c**, cytochrome *c* 10 µM; test for mitochondrial outer membrane integrity. **3U4.5**, uncoupler titrations to optimum CCCP concentration 4.5 µM; NADH-linked ET capacity N_E. **4G**, glutamate 10 mM; N(PGM)$_E$. **5S**, succinate 10 mM; NS-pathway ET capacity, NS_E. **6Oct,** octanoylcarnitine 0.5 mM; FNS-pathway ET capacity, FNS_E. **7Rot**, rotenone 0.5 µM inhibiting CI; succinate-pathway ET capacity S_E. **8Gp**, glycerophosphate 10 mM; SGp_E. **9Ama**, antimycin A 2.5 µM inhibiting CIII; residual oxygen consumption *Rox*.

10AsTm, ascorbate 2 mM & TMPD 0.5 mM; substrates for CIV stimulation; the chamber was kept open for 20 min to allow for redox equilibration without depletion of oxygen [Doerrier et al 2018]; O_2 flux (107 pmol·s^{-1}·mL^{-1}) off scale after closing the chamber. **11Azd**, azide 200 mM inhibiting CIV; oxygen-dependent chemical background flux *Chb*. **(b)** and **(d)** RP2 (SUIT-002_D007): **ce1**, *R*. **+Dig**, *Ren*. **+D**, stimulating *Ren*. **+M.1**, malate 0.1 mM and **1Oct**, octanoylcarnitine; F-pathway OXPHOS capacity $F_P = J(1Oct)\text{-}J(+M.1)$. **1c**. **2M2**, malate 2 mM supporting the anaplerotic N-pathway; $F(N)_P$. **3P** and **4G**, progressive activation to FN_P. **5S**, FNS_P. **6Gp**, $FNSGp_P$. **7U4.5**, uncoupler titrations to optimum CCCP concentration 4.5 µM; $FNSGp_E$. **8Rot**, SGp_E. **9Ama**, *Rox*. **10AsTm**, O_2 flux off scale 121 pmol·s^{-1}·mL^{-1}. **11Azd**, *Chb*. In general, Complex IV activity is the difference of rates, J(10AsTm)-J(11Azd) at closely matched O_2 concentrations. In RP1 and RP2, *identical* respiratory states are shown by green circles (ce1, *R)* and yellow circles (+Dig, *Ren*); *harmonized* respiratory states are shown by blue circles (8Gp and 8Rot, SGp_E) and pink circles (J(10AsTm)-J(11Azd), CIV). Count concentration of cells: 1 million per mL. Data repository: RP1 (2021-11-16_P3-02) and RP2 (2021-11-17_P2-02).

2.5. Data analysis

O_2 fluxes, corrected for instrumental O_2 background, were computed (DatLab 7.4 and 8.1, Oroboros Instruments, Austria) as the medians of data points within marked sections. The measured O_2 fluxes were not baseline-corrected for *Rox* obtained after inhibition by Ama. *Rox* averaged 0.5 % of flux in steps 6Oct (FNS_E) or 7U ($FNSGp_E$) in RP1 and RP2, respectively (Figure 2a and 2b). In several individual assays, *Rox* was close to zero below the limit of detection, with consistently low averages ranging from -0.1 % to 0.9 % for the lots of MiR05-Kit and 0.1 % to 1.0 % for years of measurement. For CIV activity determination, fluxes were corrected for chemical background *Chb*: the flux measured after inhibition by Azd was subtracted from the total O_2 flux measured before CIV inhibition (AsTm) at practically identical O_2 concentrations.

Data were analyzed with GraphPad Prism 9 software and Microsoft Excel version 2401. Mean inverted regression lines in Figure 6 were calculated by inverted regression analysis (Gnaiger 2021). In regressions between variables in X and Y with identical errors of measurement, the ordinate Y/X slope b_Y is underestimated compared to the inverted X/Y slope b_X calculated from the abscissa X/Y slope β_X. To minimize the residuals of both variables, Y and X, slopes b_Y and β_X and intercepts a_Y and α_X are calculated for the Y/X and X/Y inverted linear regressions, respectively. The mean slope $\bar{b} = (b_Y+b_X)/2$ and mean intercept $\bar{a} = (a_X+a_Y)/2$ are used, where $b_X = 1/\beta_X$ and $a_X = -\alpha_X/\beta_X$.

Outliers (Figure 3c and 4b) were identified by calculating the mean ($\bar{x}$) and standard deviation (SD) of all data sets for each state and protocol, independent of the different lots of the MiR05-Kit. Values falling outside the range of $\bar{x} \pm 3 \cdot SD$ were classified as outliers.

For each year of measurement, the index of variation of O_2 fluxes [%] (Figure 5) was calculated for each respiratory state in the two protocols as $100 \cdot SD/\bar{x}$. The values obtained for each lot of MiR05-Kit were then averaged within a year and the corresponding standard error of the mean (SEM) was calculated.

3. Results

3.1. Cell and mitochondrial respiration

The quality of six lots of MiR05-Kit and the effect of their storage times from one to four years was evaluated by measuring the respiration in living and permeabilized cells using the SUIT protocols RP1 and RP2. We compared two (2019) or four (2020 to 2022) lots of MiR05-Kit with storage times of up to 51 months. The same batch of HEK 293T cells was used in each year of measurement to eliminate the effect of batch-to-batch variability (Table 2). Experiments with RP1 and RP2 were performed on the same day in 2019, three days apart in 2020, and on two consecutive days in 2021 and 2022.

In Figure 3, O_2 flow normalized per cell count is represented for the four comparable respiratory states in RP1 and RP2: ROUTINE respiration of living cells, residual endogenous respiration, SGp_E, and CIV activity (Figure 2a and 2b). Since different batches of cells were used for each experimental year, the lots of MiR05-Kit can only be compared within the same year. In each year of measurement, i.e. for each batch of HEK cells, respiration was independent of the MiR05-Kit lot and its storage time. These results demonstrate that MiR05-Kit was stable for up to 51 months of storage (lot #1 in 2020).

Comparing different batches of HEK cells, ROUTINE respiration was lower in HEK 2019 and HEK 2022 compared to HEK 2020 and HEK 2021. In HEK 2022, SGp_E was lower while CIV activity was higher compared to the other years, despite the correction for chemical background (Section 3.2). Except for SGp_E in the year 2021, respiratory rates in comparable states were identical in RP1 and RP2. Two outliers were identified in 2021 (red circle, Figure 3c; see also Figure 5e and f).

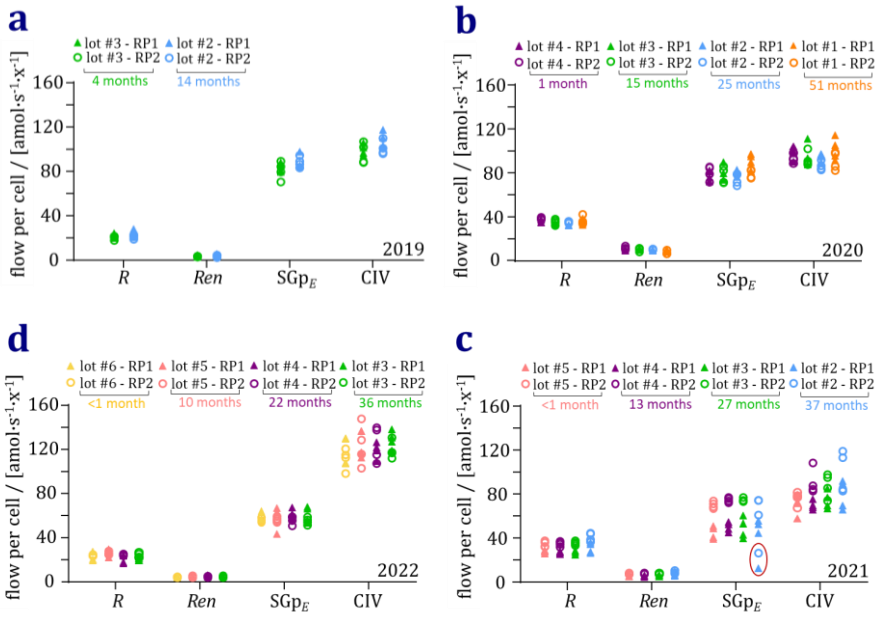

Figure 3. Respiration of HEK 293T cells in the lots of MiR05-Kit with storage times of 1 to 51 months. Two lots compared in 2019 (**a**) and four lots in 2020 to 2022 (**b** to **d**). Each panel shows O_2 flow per cell obtained in a year of measurement with the same batch of HEK 293T cells. Different batches were used in different years. In each year, respiration was not different for each respiratory state, indicating comparability between the lots of MiR05-Kit and MiR05-Kit storage times. ROUTINE and REN respiration (*R* and *Ren*, respectively) are identical in SUIT protocols RP1 and RP2, whereas respiration supported by succinate and glycerophosphate SGp_E and CIV activity refers to harmonized states in RP1 (triangles) and RP2 (circles). Symbols with the same color and shape represent technical repeats, addressing reproducibility. In 2021 (**c**), two outliers are identified for SGp_E (red circle).

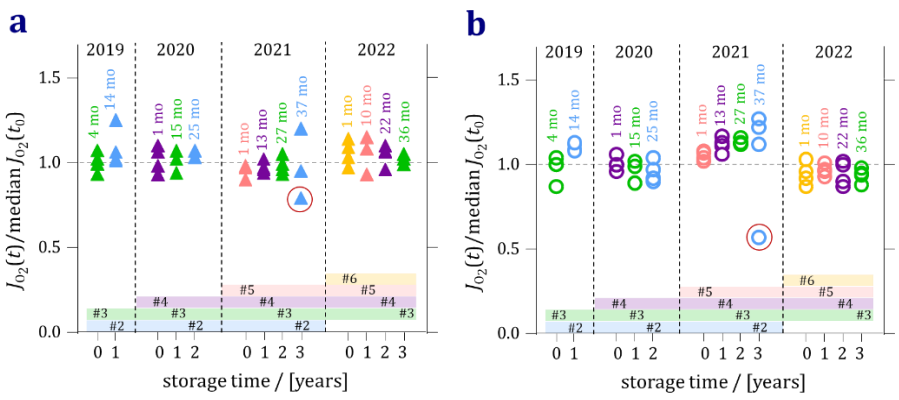

Figure 4. OXPHOS capacity of permeabilized HEK 293T in five lots of MiR05-Kit as a function of storage time. (a) PMC_P in RP1 (step 2c; triangles) and **(b)** OctPMC_P in RP2 (step 3P; circles). Flow per cell $J_{O_2}(t)$ [pmol·s^{-1}·x^{-1}] measured in the lots of MiR05-Kit at MiR05-Kit storage time t (close to 0, 1, 2, or 3 years) divided by the median flow at the shortest storage time $J_{O_2}(t_0)$, where t_0 is identified as 0 years (lot #3 in 2019, #4 in 2020, #5 in 2021 and #6 in 2022). Outliers previously identified (Figure 3c; lot#2) are marked by a red circle. Respiration was constant over storage time for each lot of MiR05-Kit, with a large scatter for the data after 37 months of storage (t_3 in 2021). Lot #1 was excluded from the analysis, as it was only used in one year of measurement.

To further evaluate the quality of the lots of MiR05-Kit and the possible effect of their storage time on respiration, the analysis was extended to OXPHOS capacity *P*. In RP1 N-OXPHOS capacity was represented by PMC_P, in the presence of pyruvate, malate, and cytochrome *c* (Figure 2c, step 2c). In RP2 FN-OXPHOS capacity was represented by OctPMC_P in the presence of octanoylcarnitine, pyruvate, malate, and cytochrome *c* (Figure 2d, step 3P). In each year of measurement, the storage time *t* of the different lots of MiR05-Kit was approximately 0 (fresh lot), 1, 2, or 3 years (Figure 4). Respiration at storage time *t*, $J_{O_2}(t)$, was divided by the median of respiration at the shortest storage time t_0, $J_{O_2}(t_0)$, within the same year. This allows the comparison between measurements in different years by removing the effect of cell-to-cell variability. Respiration was constant over increasing storage times. Similar results were obtained for all lots within the same year and between years. This confirms the stability of MiR05-Kits for a storage time of up to 36 months (lot #3 in 2022). One outlier was identified in lot #2 in 2021 (Figure 4b), within the same dataset as one of the previously identified outliers (Figure 3c).

In Figure 5, all states covered by RP1 and RP2 were analyzed separately for each year and protocol. Each panel shows results from measurements performed on the same day with subsamples of the same batch of HEK 293T cells. The median rate of O_2 consumption in each respiratory state is represented for separate lots of MiR05-Kit. The two data sets related to the previously identified outliers (Figures 3c and 4b) were plotted separately (lot #2, Figure 5e and 5f). These data sets were obtained in the same Oroboros chamber (P1A, chamber A of O2k P1) on consecutive days (RP1 and RP2, respectively). In these chambers, the flow per cell was low in all respiratory states after the addition of cytochrome *c*, providing evidence for the classification of these two whole data sets as outliers (Section 4). The average index of variation over all years of measurement with lots #1 to 6 of MiR05-Kit was 7.5 % with average SEM of 1.5 for ROUTINE respiration as the first respiratory step of the protocols, and 6.9 % with average SEM of 1.4 for steps 6Oct and 7U in RP1 and RP2, respectively, as late steps in the protocol with maximum O_2 flux.

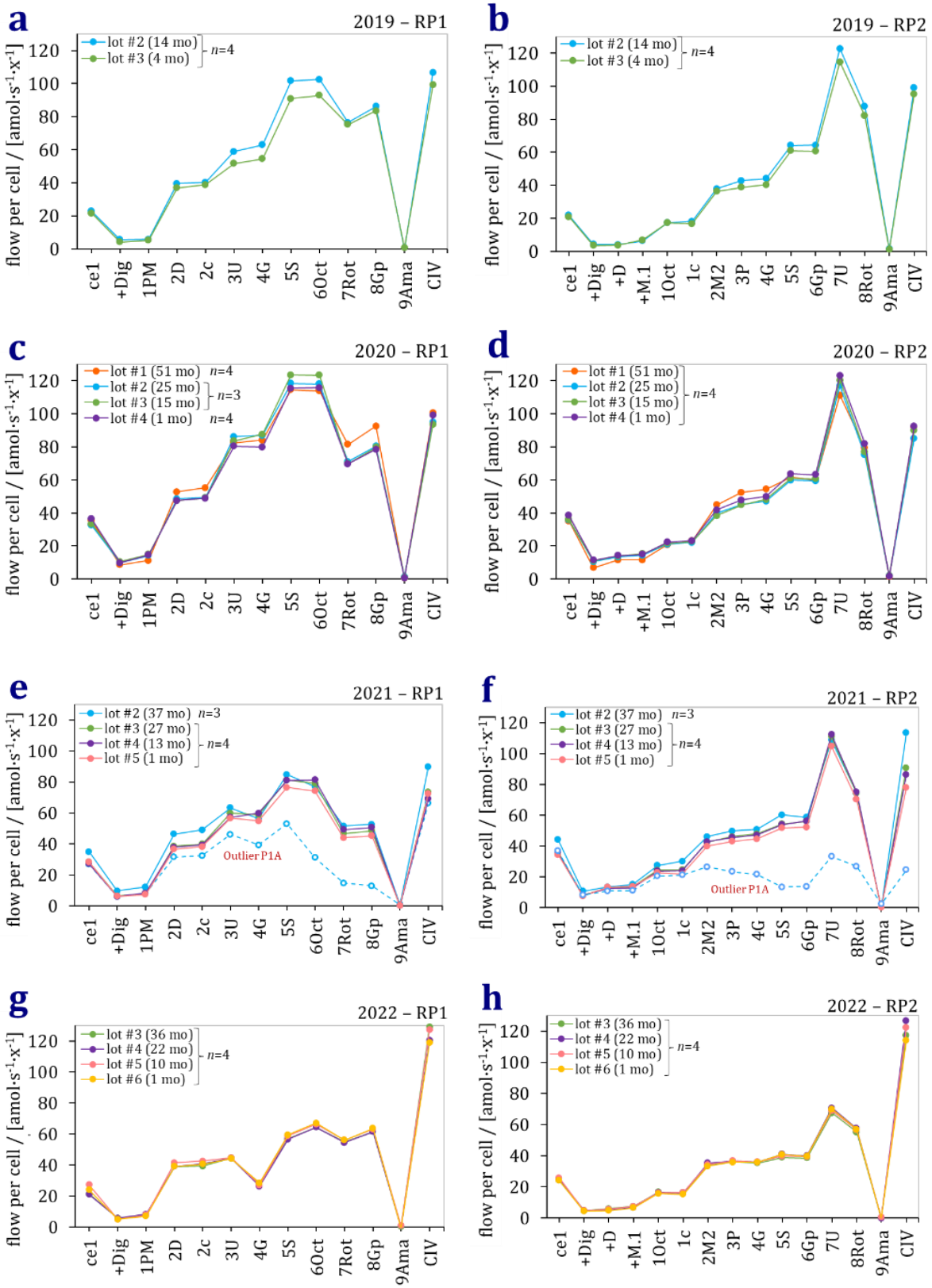

Figure 5. Respiration in the lots of MiR05-Kit with different storage times. Each panel shows parallel measurements performed on the same day with subsamples from the same batch of HEK 293T cells. Respiratory states are identified on the *X*-axis according to Figure 2 (RP1 and RP2). CIV activity is calculated as the rate in state AsTm corrected

for chemical ROX (Azd). Each dot indicates the median of flow per cell of *n* technical repeats obtained with the same lot of MiR05-Kit. In panels **e** and **f**, the dashed line represents a specific measurement with lot #2 identified as outliers (O2k P1, chamber A). Comparable results are obtained with different lots of MiR05-Kit for each year.

Taken together, there was no effect on respiration of the different lots of MiR05-Kit nor their storage times throughout the protocols when evaluated within the same year of measurement. Therefore, the results of the present long-term study were used for comparison of different batches of HEK 239T cells. For each year of measurement (batch of HEK cells; Table 2) and comparable respiratory state, respiration in RP1 was plotted in relation to respiration in RP2 measured in the same Oroboros chamber (Figure 6a). RP1 and RP2 were measured on two experimental days (1 to 3 days apart) from 2020 to 2022, but in parallel on the same day in 2019. Therefore, 2019 data were only represented as averages in Figure 6b. Different batches of HEK cells show separate clusters. In 2020 and 2022, these clusters are arranged along an identical regression line (isolinearity). In this case, the comparable respiratory states gave results in both protocols close to the theoretical line of correspondence. In 2021, however, the clusters follow a different regression line compared to the other years. The generally higher respiration rates observed in RP2 could not be explained by different cell viabilities on the consecutive days of measurement (Table 2). However, it can be hypothesized that either the cell count was underestimated or respiratory activity per cell was higher in the cryovials on the second day, with vials for both days obtained from the same cell culture used for cryopreservation (Section 4).

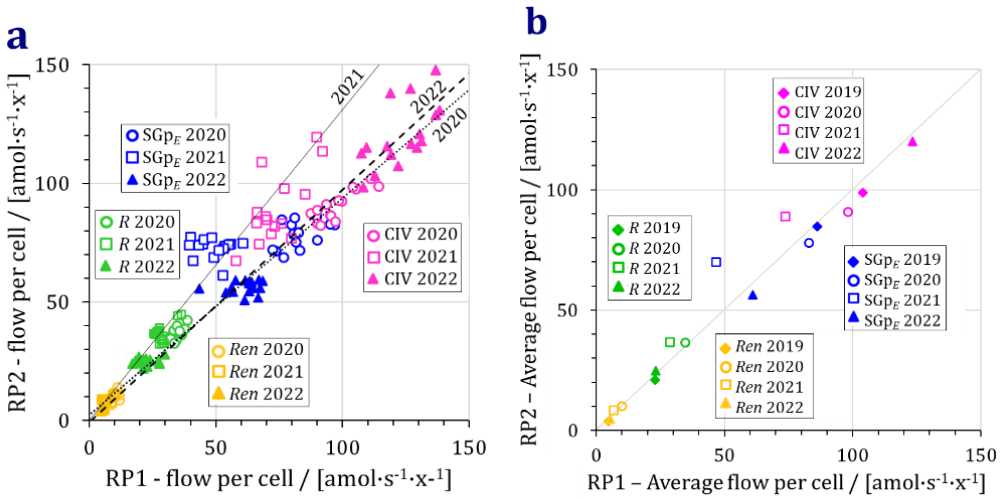

Figure 6. Bioenergetic cluster analysis of respiration in comparable respiratory states in RP2 versus RP1. RP1 and RP2 were performed on the same day (2019) and 3 (2020) or 1 days apart (2021 and 2022). **(a)** Separate clusters identified for different batches of HEK cells. The isolinearity of the clusters is indicated by regression lines (dotted, full and dashed, for 2020, 2021 and 2022 respectively). In 2021, the clusters are arranged along a different regression line compared to the other years. Regression lines are calculated by inverted regression analysis; 2020: $y = 1.31x + 0.02$ (r^2= 0.98), 2021: $y = 0.91x + 2.51$ (r^2= 0.93), 2022: $y = 0.98x - 0.58$ (r^2= 0.98). The two outliers in SGp_E state for 2021 in the same Oroboros chamber (Figure 5) lead to an outlier point which was eliminated from the graph as it provides no further information. **(b)** Flow per cell represented as average for each comparable respiratory state. The grey line represents the line of identity ($y=x$).

3.2. Chemical O_2 background test

CIV activity was measured in the presence of cytochrome *c* after inhibition of Complex III with antimycin A. O_2 flux was stimulated by ascorbate and TMPD (Figure 2; 10AsTm). This was followed by inhibition of CIV by Azd to quantify the chemical background flux *Chb* of autoxidation. To eliminate any possible effect of the sample, autoxidation of cytochrome *c*, ascorbate, and TMPD was measured in chemical O_2 background tests performed in the absence of sample in parallel to the cellular experiments in 2020, 2021 and 2022.

Autoxidation is accelerated by transition metals. Therefore, the chemical O_2 background test constitutes a quality control for the purity of the MiR05-Kit powder or the finally prepared MiR05 solution. Autoxidation is a linear function of O_2 concentration above 50 µM while it transitions to a hyperbolic function in the low-oxygen region (Kuznetsov, Gnaiger 2015). To restrict the analysis to the region of linear oxygen-dependence, marks from Tm1 to Tm10 were set on the plot of O_2 flux per *V* ($J°'_{O2}$) in the range of corresponding O_2 concentrations above 50 µM (Figure 7). Based on these marks, the intercept at zero-oxygen $a°'$ and the slope $b°'$ of the linear regression were calculated for each individual experiment (Supplement S1). $J°'_{O2}$ was then expressed at 180 µM (near air saturation), 50 µM (low O_2 concentration in the linear range of oxygen-dependence), and by extrapolation as the intercept at 0 µM ($a°'$; Figure 8).

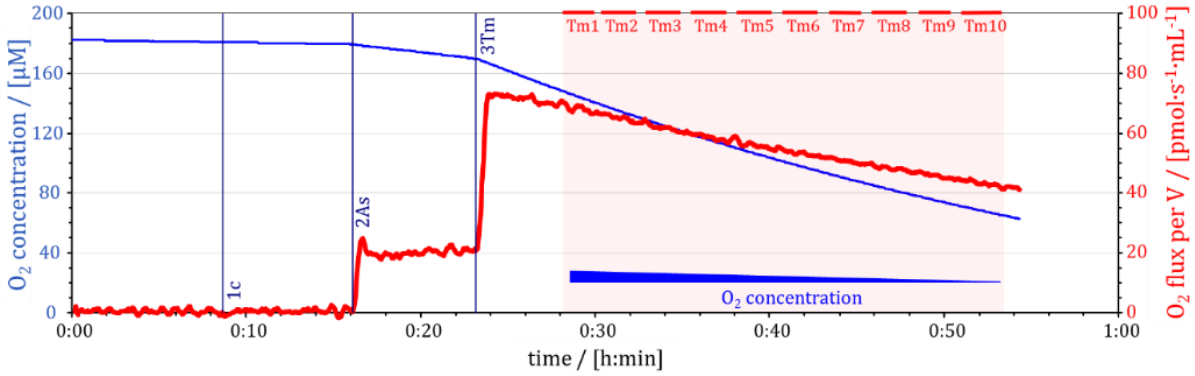

Figure 7. Representative HRR trace for evaluation of autoxidation as a chemical quality control of MiR05. Measurement in MiR05 with 10 µM cytochrome *c*, 2 mM ascorbate, and 0.5 mM TMPD, without catalase. The volume-specific O_2 flux (red line) was corrected for instrumental background O_2 flux. The recording was stopped at 50 µM O_2, restricting the measurement to the region of linear oxygen-dependence below which there is a hyperbolic decline of autoxidation towards zero-oxygen. Ten marks (red bars) were set in this linear region (red shade). Autoxidation is used for chemical O_2 background correction. Data repository: 2021-11-19_P1-02.

Years 2020 and 2021 show comparable values for all three O_2 concentrations, with a slight aging effect related to the storage time of the MiR05-Kit, especially visible for lot #2 in 2021 (Figure 8a and b). The most evident result is the difference of $J°'_{O2}$ values in 2022, which are significantly higher for all O_2 concentrations compared to previous years (highlighted by the need for a different *Y*-axis scale in Figure 8c). This discrepancy was not linked to differences between the lots of MiR05-Kit and thus is related to the chemicals titrated (Figure 7).

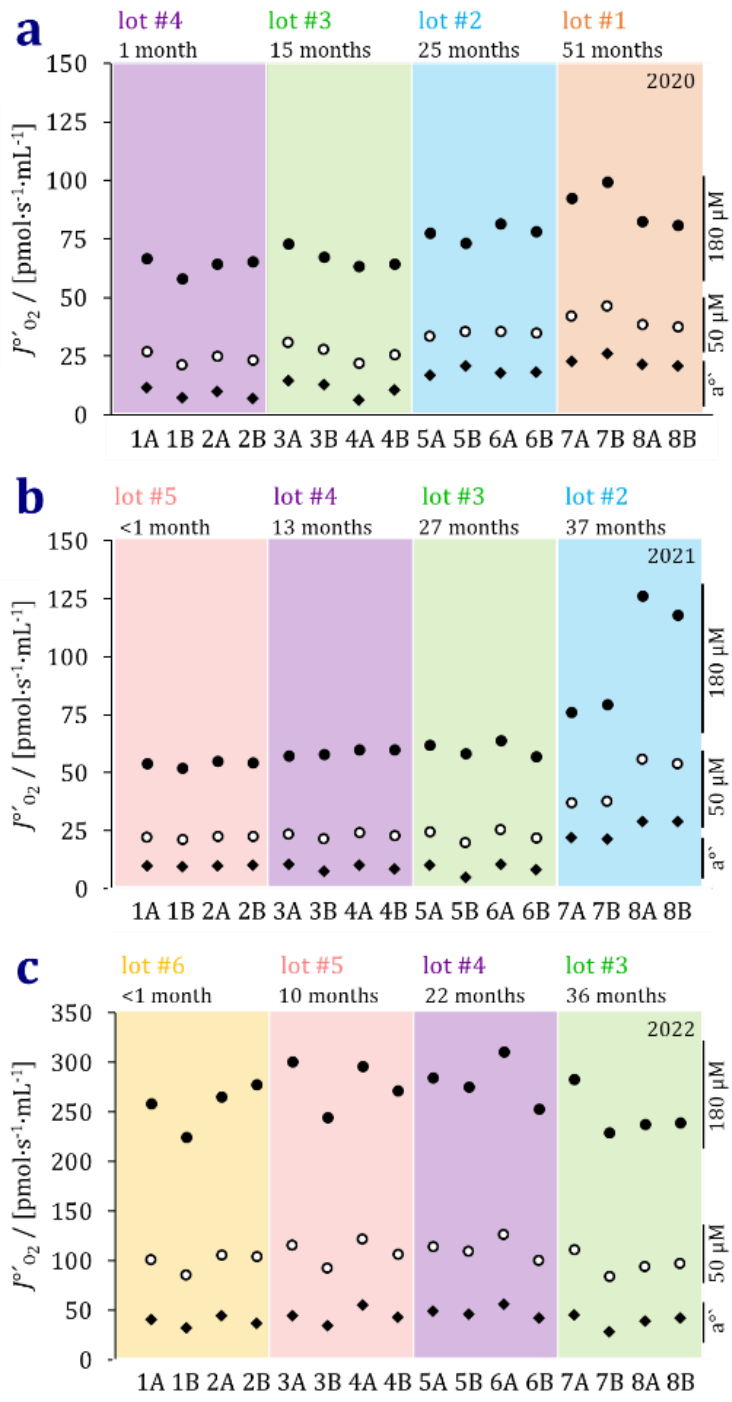

Figure 8. Chemical O_2 background flux $J'°_{O2}$ at different O_2 concentrations. For each year, $J'°_{O2}$ of 8 Oroboros with chambers A and B, represented by numbers from 1A to 8B, was measured with the protocol shown in Figure 7. $J'°_{O2}$ at a given O_2 concentration was calculated from the parameters $a°'$ (intercept at 0 µM O_2, diamonds) and the slope $b°'$ for 50 µM (low O_2 concentration in the linear range of oxygen-dependence, open circles) and 180 µM (near air saturation, closed circles). These $J'°_{O2}$ values were independent of the lot of MiR05-Kit, with a slight aging effect related to the storage time in 2020 and 2021. In 2022 values are much higher in respect to the other years. The chemical O_2 background test was not performed in 2019.

4. Discussion

Mitochondrial respiration media are classically either KCl-based with 0.15 M KCl or sucrose-based with 0.25 M sucrose (Reynafarje et al 1985). With reference to organ storage solutions with an intracellular formulation (University of Wisconsin solution; ViaSpan; Du Pont), mitochondrial respiration medium MiR05 has been developed to avoid a high Cl^- concentration by using K-lactobionate and reducing the sucrose concentration (Gnaiger et al 2000). In sucrose-based solutions, coupling between respiration and ATP production is tighter compared to KCl-based media (Manko 2013). Several studies on media containing both sucrose and K-lactobionate demonstrate their ability to maximize ADP-stimulated respiration of isolated mitochondria (Wollenman 2017) and to stabilize membrane-bound cytochrome *c* (Gnaiger et al 2000), thanks to the lack of a high Cl^- concentration. In addition, MiR05 is advantageous in fluorespirometric applications of Amplex UltraRed for the measurement of hydrogen peroxide production (Komlódi et al 2018; 2021; Krumschnabel et al 2015). Moreover, a recent study comparing respiration of human skeletal muscle fibers in MiR05

and medium Z demonstrates that mitochondrial respiratory capacities are higher in MiR05 at high-oxygen regimes than in medium Z near air saturation (Doerrier et al 2024).

We replaced our laboratory-based preparation of MiR05 by using MiR05-Kit. The reproducible results obtained in experiments with six lots of MiR05-Kit, stored at room temperature for different periods, demonstrate the consistency between the lots and stability of the MiR05-Kit for storage times up to 51 months. Over the 4-year study with a total of 110 experiments, only two outliers were identified (Figure 5e and 5f). Compared to the other results, these outliers presented a much lower respiration starting from states 2D and 1c in RP1 and RP2, respectively. These measurements were conducted in the same Oroboros chamber on consecutive days, which suggests a possible contamination in the chamber. Carryover of inhibitors from previous experiments, for example, rotenone, may cause decreased O_2 flux. However, this should have also affected ROUTINE respiration, which shows instead expected values for the outliers. Moreover, rotenone titration showed an inhibitory effect in both measurements. The presence of the outliers seems, therefore, to be related to multiple effects rather than caused by a single inhibitor.

Besides these outliers, a different trend was identified in 2021 in comparison to the other years of measurement. In fact, respiration in the comparable respiratory states showed higher values in RP2 than in RP1, resulting in a correlation line shifted from the line of identity (Figure 6). This difference was already apparent in the initial ROUTINE state. Considering that the experiments in RP1 and RP2 were performed with two subsamples of the same batch of cells, several biological and operational causes can be addressed. Even if cell viability did not show significant differences (Table 2), the cell count procedure or the addition of the sample to the Oroboros chambers on the second day represent possible sources of error. Moreover, differences in mitochondrial content could have affected the results.

In general, cell-to-cell variability is an essential element to consider when performing prolonged studies, especially if several batches of cells are used in different years of measurement. We cannot exclude that the number of passages in the range of 3 to 10 might explain some variability in respiratory capacities between years of measurement. In fact, this may lead to differences in the O_2 fluxes in corresponding states of the same protocol measured with different batches of cells. Some examples are visible in Figure 5: in RP1, ET states after addition of succinate (5S) and octanoylcarnitine (6Oct) vary from rates below 70 amol·s^{-1}·x^{-1} (2022, Figure 5g), reaching values above 110 amol·s^{-1}·x^{-1} (2020, Figure 5c); RP2 shows instead a much lower ET capacity in 2022 (7U, Figure 5h) compared to the other years of measurement, with a maximum of median respiration of 70 amol·s^{-1}·x^{-1}. For a correct interpretation of these results, it must be considered that not only different batches of HEK cells were used, but also different batches of SUIT chemicals, which may have affected the response in respiration.

CIV activity, obtained as the difference of flux in the AsTm and Azd steps in both protocols, presents a higher variability, within the same year and between years (Figure 6a). This is especially evident in 2022, where CIV reaches fluxes up to 130 amol·s^{-1}·x^{-1}, compared to the maximal 100 amol·s^{-1}·x^{-1} in other years (Figure 5). This difference was consistent with the chemical background O_2 flux, generally higher in 2022 for all O_2 concentrations (Figure 8). Our analyses suggest that this abnormality was related to SUIT chemical QC rather than MiR05.

5. Conclusions

Over this 4-year study, we evaluated the stability of mitochondrial respiration medium MiR05, prepared from six different lots of MiR05-Kit. In each year of measurement, different lots had storage times at room temperature from 1 to 51 months. The study aimed to assess whether the increasing storage time of the MiR05-Kit has an effect on its functionality and on the quality of the obtained results.

The analysis, carried out with SUIT reference protocols RP1 and RP2 and cryopreserved HEK cells, demonstrates that no significant difference in the respiration is observed in relation to the lots of MiR05-Kit and their varying storage time. Moreover, the analysis of chemical background O_2 flux, performed as a chemical test for the autoxidation of the components of the MiR05-Kit, confirmed the stability of the MiR05-Kit up to 51 months of storage time.

In conclusion, these results are essential to prove the constant quality of MiR05-Kit across different lots and storage times, for a period of time exceeding the expiration date. This represents a key element in supporting the choice of MiR05-Kit for preparation of a standardized respiration medium, to guarantee reliability and consistency of the results in mitochondrial research.

Abbreviations

BSA	bovine serum albumin	MiR05-Kit	powder of main components of MiR05
Chb	chemical background		
CR	cryopreservation	O_2	oxygen
ET	electron transfer	*P*	OXPHOS capacity
HRR	high-resolution respirometry	QC	quality control
MiR05	mitochondrial respiration medium prepared from MiR05-Kit	RP	reference protocol
		SUIT	substrate-uncoupler-inhibitor titration

Acknowledgements

We thank Omar Torres-Quesada, Institute of Biochemistry, University of Innsbruck for providing the HEK cells. This work was partially funded by the European Union's Horizon 2020 research and innovation program under grant agreement No. 859770, NextGen-O2k project.

References

Doerrier C, Gama-Perez P, Pesta D, Distefano G, Soendergaard SD, Maise Chroeis K, Gonzalez-Franquesa A, Goodpaster BH, Prats C, Sales-Pardo M, Guimera R, Coen PM, Gnaiger E, Larsen S, Garcia-Roves PM (2024) Harmonization of experimental procedures to assess mitochondrial respiration in human permeabilized skeletal muscle fibers. https://doi.org/10.1016/j.freeradbiomed.2024.07.039

Doerrier C, Garcia-Souza LF, Krumschnabel G, Wohlfarter Y, Mészáros AT, Gnaiger E (2018) High-Resolution FluoRespirometry and OXPHOS protocols for human cells, permeabilized fibers from small biopsies of muscle, and isolated mitochondria. https://doi.org/10.1007/978-1-4939-7831-1_3

Gnaiger E (2008) Polarographic oxygen sensors, the oxygraph and high-resolution respirometry to assess mitochondrial function. In: Mitochondrial dysfunction in drug-induced toxicity (Dykens JA, Will Y, eds) John Wiley & Sons, Inc, Hoboken, NJ:327-52.

Gnaiger E, Kuznetsov AV, Schneeberger S, Seiler R, Brandacher G, Steurer W, Margreiter R (2000) Mitochondria in the cold. In: Life in the Cold (Heldmaier G, Klingenspor M, eds) Springer, Berlin, Heidelberg:431-42. https://doi.org/10.1007/978-3-662-04162-8_45

Gnaiger E (2021) Bioenergetic cluster analysis – mitochondrial respiratory control in human fibroblasts. https://doi.org/10.26124/mitofit:2021-0008

Komlódi T, Sobotka O, Gnaiger E (2021) Facts and artefacts on the oxygen dependence of hydrogen peroxide production using Amplex UltraRed. https://doi.org/10.26124/bec:2021-0004

Komlódi T, Sobotka O, Krumschnabel G, Bezuidenhout N, Hiller E, Doerrier C, Gnaiger E (2018) Comparison of mitochondrial incubation media for measurement of respiration and hydrogen peroxide production. https://doi.org/10.1007/978-1-4939-7831-1_8

Krumschnabel G, Fontana-Ayoub M, Sumbalova Z, Heidler J, Gauper K, Fasching M, Gnaiger E (2015) Simultaneous high-resolution measurement of mitochondrial respiration and hydrogen peroxide production. https://doi.org/10.1007/978-1-4939-2257-4_22

Krumschnabel G, Lamberti G, Hiller E, Hansl M, Gnaiger E (2024) Development of a reference sample for high-resolution respirometry. Version 3. https://wiki.oroboros.at/index.php/MiPNet21.14_Reference_sample_HRR

Kuznetsov AV, Gnaiger E (2015) Oxygraph assay of cytochrome *c* oxidase activity: chemical O_2 background correction. https://wiki.oroboros.at/index.php/MiPNet06.06_Chemical_O2_background

Leo E, Rychtarova L, Garcia-Souza LF, Åsander Frostner E, Elmér E, Gnaiger E (2024) High-resolution respirometry in a small-volume chamber. https://doi.org/10.26124/mitofit:2024-0004.v2

Manko BO, Klevets MY, Manko VV (2013) An implication of novel methodology to study pancreatic acinar mitochondria under in situ conditions. https://doi.org/10.1002/cbf.2864

Reynafarje B, Costa LE, Lehninger AL (1985) O_2 solubility in aqueous media determined by a kinetic method. https://doi.org/10.1016/0003-2697(85)90381-1

Timón-Gómez A, Doerrier C, Sumbalová Z, Garcia-Souza LF, Baglivo E, Cardoso LHD, Gnaiger E (2024) Analysis of mitochondrial respiratory pathway and coupling control by substrate-uncoupler-inhibitor titration reference protocols. https://doi.org/10.26124/mitofit:2024-0008

Wollenman LC, Vander Ploeg MR, Miller ML, Zhang Y, Bazil JN (2017) The effect of respiration buffer composition on mitochondrial metabolism and function. https://doi.org/10.1371/journal.pone.0187523

Supplement S1

The autoxidation of cytochrome *c*, ascorbate and TMPD in the absence of sample can be evaluated in chemical O_2 background tests. For O_2 concentrations above 50 µM, the relationship between O_2 concentration and chemical O_2 background flux $J°'_{O2}$ can be expressed as a linear regression. The values of the intercept at zero-oxygen $a°'$ and the slope $b°'$ were calculated by setting ten marks (Tm1 to Tm10, Figure 7) on the plot of O_2 flux per V. For each mark, $J°'_{O2}$ was plotted as a function of the corresponding O_2 concentration, and the equation of the regression line calculated using Excel ($y = b°'x + a°'$). As an example, the obtained regression lines are shown in Figure S1 for year 2022, where the measurements were performed in eight Oroboros using four lots of MiR05-Kit with storage times from 1 to 36 months. The similarity of the results indicates no effect on $J°'_{O2}$ of the different lots of MiR05-Kit and their storage times, as previously observed in Figure 8.

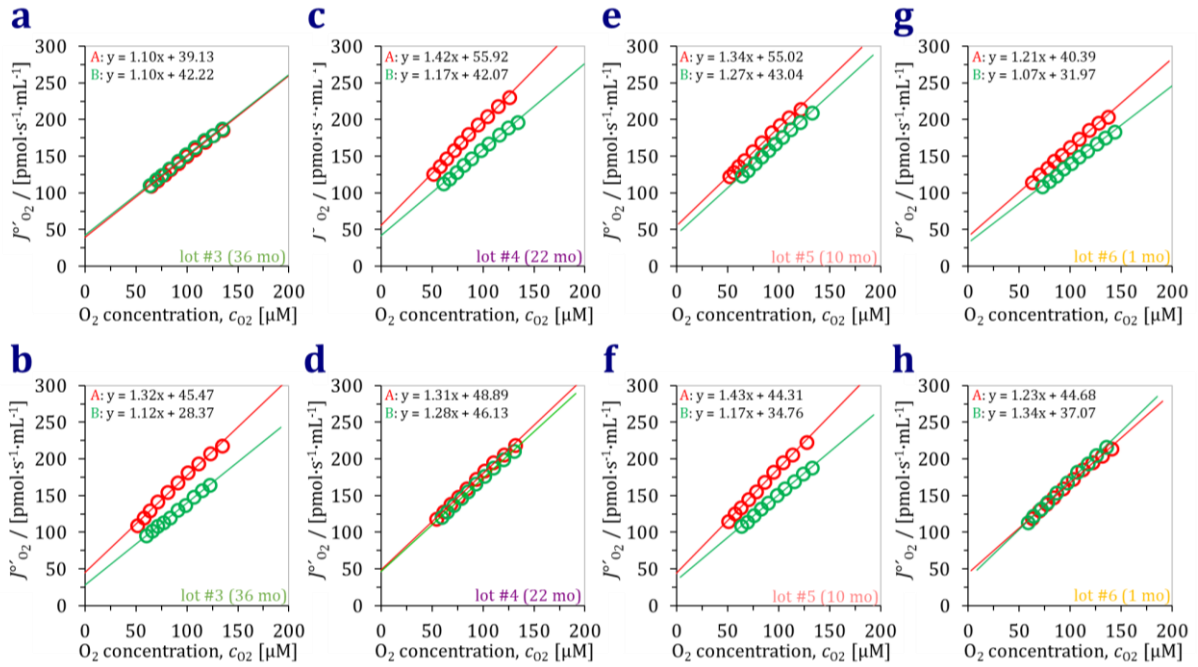

Figure S1. Analysis of chemical O_2 background with 4 different lots of MiR05-Kit in 2022. Chemical O_2 background flux $J°'_{O2}$ plotted as a function of O_2 concentration using 10 marks (Tm1 to Tm10, Figure 7) for 8 Oroboros (16 chambers; Figure 8). Regression lines are shown in each graph separately for chambers A and B (red and green lines, respectively). The intercept at zero oxygen ($a°'$), slope ($b°'$), lot number of MiR05-Kit, and storage time are shown in each panel.